a

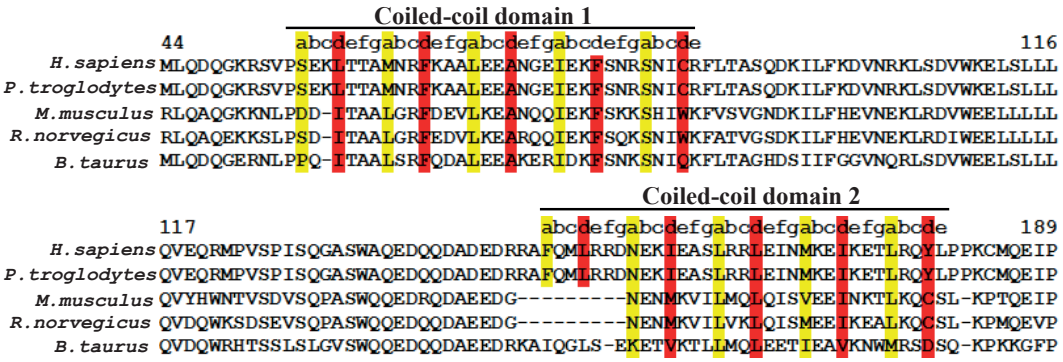

b

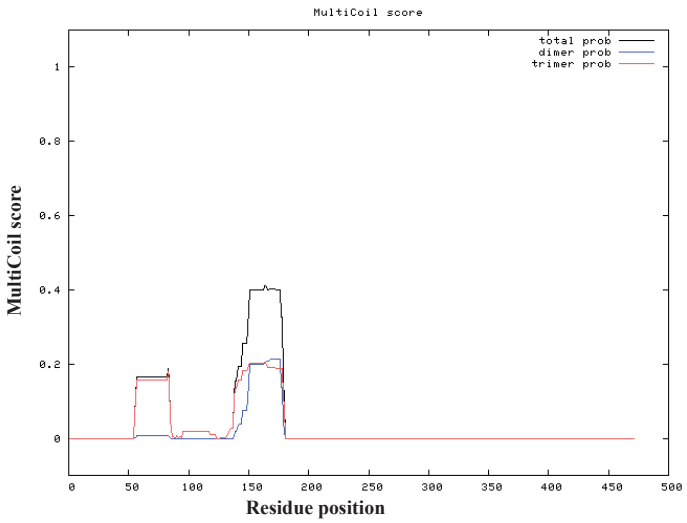

Supplementary Figure 1 Structure determination and assembly pattern prediction of coiled-coil domain, related to Figure 1. (a) Sequence alignment of the N-terminal coiled-coil domain of MLKL from vertebrate species. Two distinctive heptad repeat pattern (abcdefg)n characteristic of a coiled-coil architecture are indicated above the alignment. Coiled-coil residues occupying hydrophobic 'a' and 'd' position are denoted by yellow and red. These coiled-coil motifs are commonly shared among the MLKL orthologs in different vertebrate species. (b) Prediction of oligomerization states of coiled-coil domain of MLKL by Multicoil program (http://groups.csail.mit.edu/cb/multicoil/cgi-bin/multicoil.cgi). The score for potential coiled-coils with a dimeric probability is indicated by blue line and a trimeric probability is indicated by red line. The sum of these two probabilities is the total probability for forming a coiled-coil, which is indicated by black line.

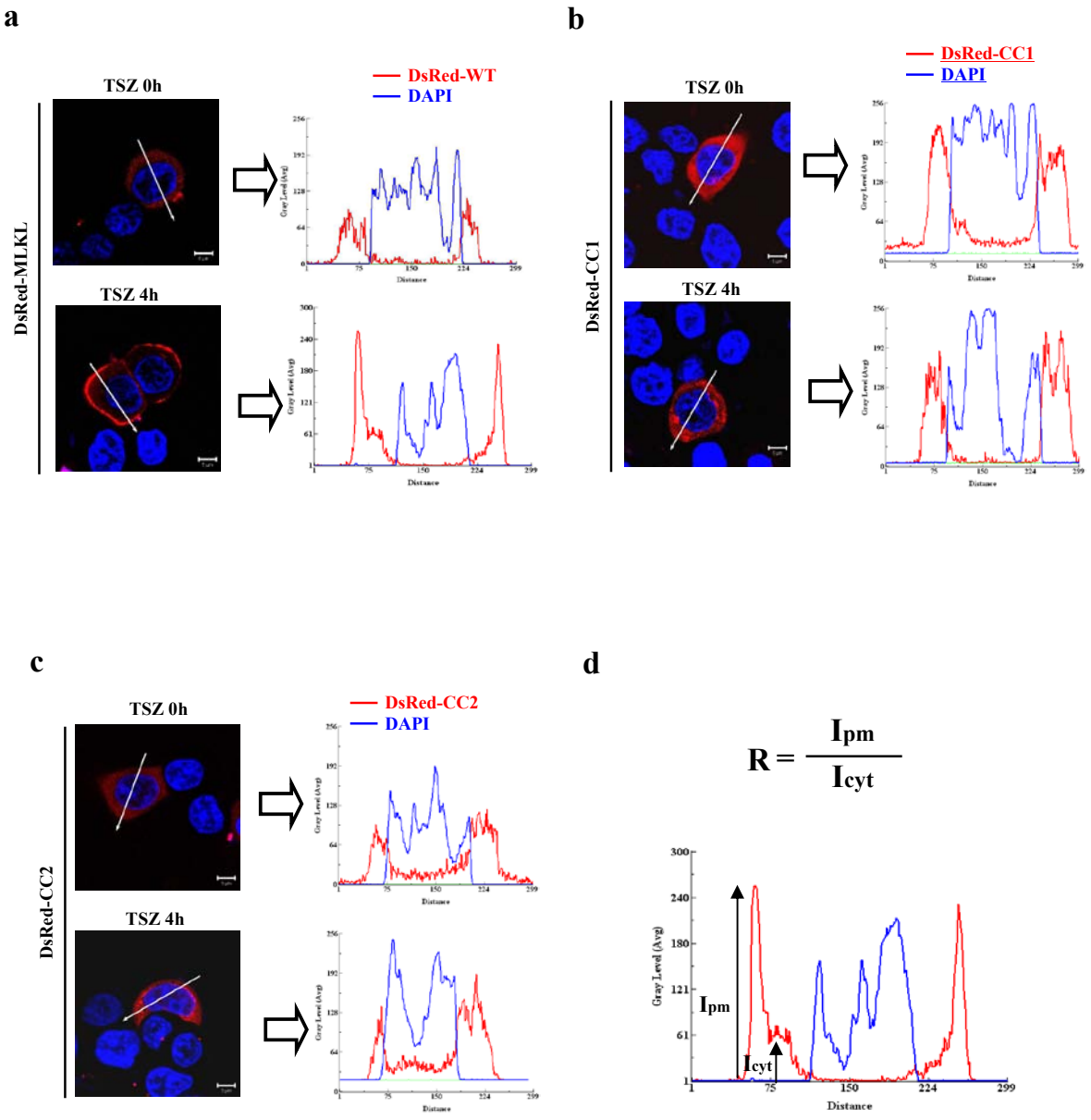

Supplementary Figure 2 Quantification of plasma membrane translocation of DsRed-MLKL in response to TSZ treatment, related to Figure 4d. (a-c) MLKL shRNA HT29 cells transfected with DsRed tagged WT MLKL (a), CC1 (b) or CC2 (c) mutants and then treated with TSZ as indicated. A line intensity profile across the cell was obtained in a given image. Representative intensity profiles are shown in the right. Y-axis, Gray level; X-axis, Line distance. (d) The image shown in (a) was used for a representative example to show how to calculate a relative ratio of flurorescence intensity between plasma membrane adjacent area and cytosolic area. The ratio [R] was calculated by dividing the plasma membrane intensity [*I*pm] by the average cytosolic fluorescence intensity [*I*cyt]. Scale bar, 5μm.

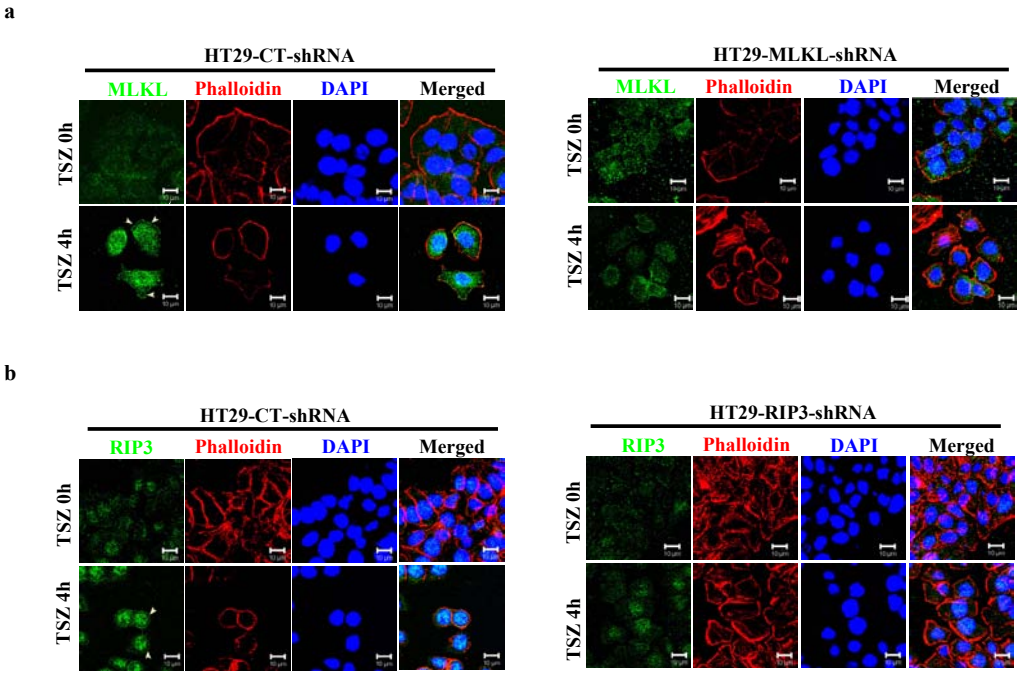

Supplementary Figure 3 Subcellular localization of endogenous MLKL and RIP3 in HT29 cells. Control shRNA (left panel) or MLKL shRNA (right panel) HT29 cells were treated with TSZ as indicated. Subcellular localization of (a) MLKL or (b) RIP3 was detected by confocal imaging of anti-MLKL antibody or anti-RIP3 antibody staining, respectively. Cell morphology was shown by F-actin probe phalloidin staining. DAPI was used for nuclear staining. White arrows indicate membrane localization. Scale bar, 10μm.

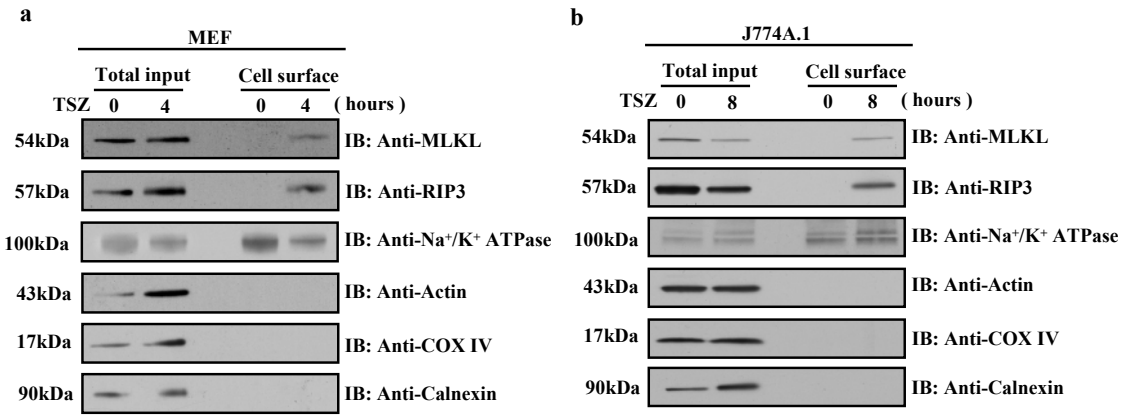

Supplementary Figure 4 Cell surface protein isolation in MEF cells and J774A.1 cells. MEF cells (a) or J774A.1 cells (b) were treated with TSZ as indicated. Total cellular lysate and the biotinylated, cell surface fraction were resolved on reducing gel and analyzed by immunoblot as indicated. Na^+/K^+ ATPase was used as a positive control for transmembrane/surface protein while Actin, COX IV and Calnexin were used as a positive control for cytosolic, mitochondrial and ER membrane proteins, respectively. Uncropped images of western blots are shown in Supplementary Fig.8.

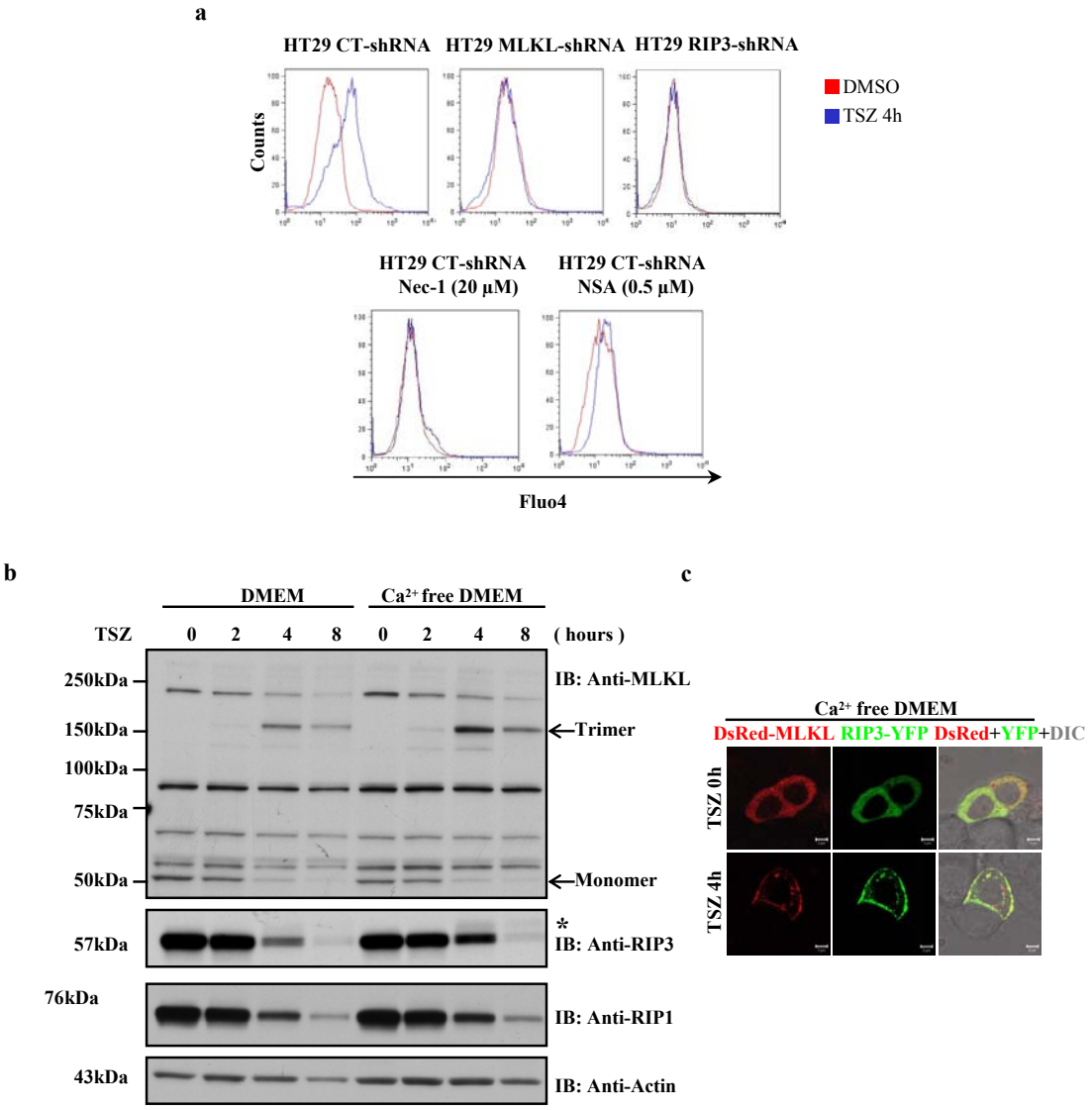

Supplementary Figure 5 MLKL-mediated Calcium influx is involved in plasma membrane rupture during necroptosis, related to Figure 6. (a) Flow cytometric analysis of intracellular Ca^{2+} of control shRNA, MLKL shRNA or RIP3 shRNA HT29 cells after treated with TSZ for 4 h with/out NSA or Nec-1 as indicated. Cells were harvested and the Fluo4 fluorescent cells were determined by FACS analysis using Fluo4. (b) HT29 cells were treated with TSZ either in normal DMEM or calcium free DMEM at different time points as indicated. The cell lysates were resolved on non-reducing gel and analyzed by immunoblot with anti-MLKL, anti RIP3, anti-RIP1 or anti-Actin antibodies. * indicates phosphorylated RIP3. (c) Representative image of live HT29 MLKL shRNA cells co-expressing DsRed-MLKL together with RIP3-EYFP treated with TSZ at time 0 and 4 hours in calcium free DMEM. Scale bar, 5μm. Uncropped images of western blots are shown in Supplementary Fig.8.

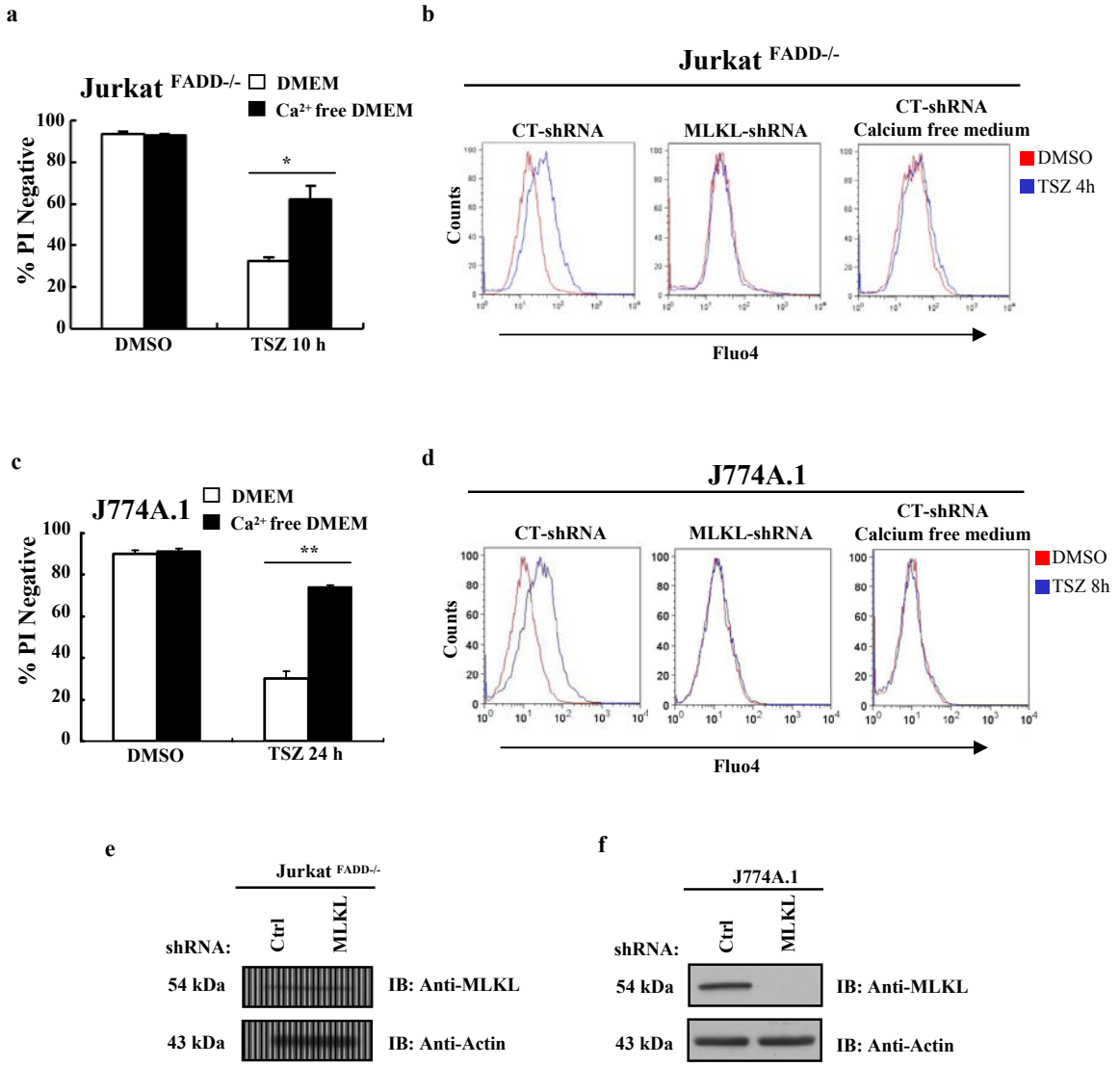

Supplementary Figure 6 Extracellular calcium is involved in necroptosis in Jurkat $^{FADD-/-}$ and J774A.1 cells. Jurkat $^{FADD-/-}$ or J774A.1 cells were cultured with/out calcium and treated with DMSO control or TSZ as indicated. (a), (c) Cell survival was determined by PI staining. Results shown are averages±S.E.M. from three independent experiments.*, $p < 0.05$, **, $p < 0.01$. Statistics source data for Supplementary Figure 6 can be found in Table S2. (b), (d) Jurkat $^{FADD-/-}$ or J774A.1 cells expressing control shRNA, MLKL shRNA or cells cultured in calcium free medium were treated with TSZ as indicated. Cells were harvested and the Fluo4 fluorescent cells were determined by FACS analysis using Fluo4. (e), (f) Immunoblot analysis of Juarkat $^{FADD-/-}$ (e) or J774A.1 (f) clones expressing control-shRNA or MLKL-shRNA with anti-MLKL or anti-Actin antibodies. Uncropped images of western blots are shown in Supplementary Fig.8.

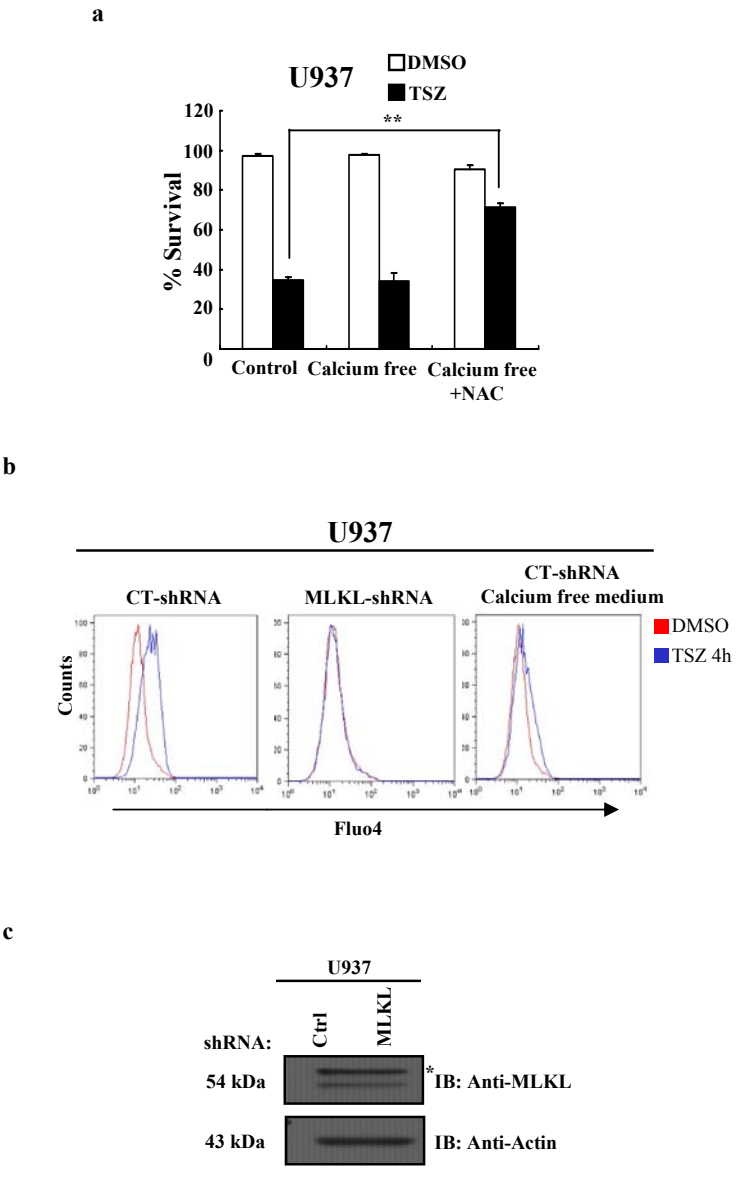

Supplementary Figure 7 ROS and calcium are both required for necroptosis in U937 cells. (a) U937 cells were either cultured in calcium free medium or cultured in calcium free medium and pre-treated with NAC (5 mM). Then, the cells were treated with TSZ. After 10 hours, cell survival was determined by PI staining. Results shown are averages of triplicates ±SEM. (b) U937 cells cultured in calcium free DMEM were treated with TSZ as indicated. Cells were harvested and the Fluo4 fluorescent cells were determined by FACS analysis using Fluo4. (c) Immunoblot analysis of U937 clones expressing control-shRNA or MLKL-shRNA with anti-MLKL or anti-Actin antibodies. * indicates non-specific band. * *, $P<0.01$. Statistics source data for Supplementary Figure 7 can be found in Supplementary Table 1. Uncropped images of western blots are shown in Supplementary Fig.8.

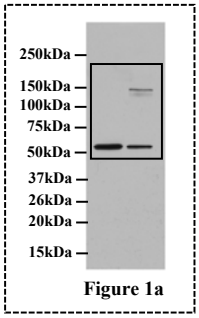

Figure 1a

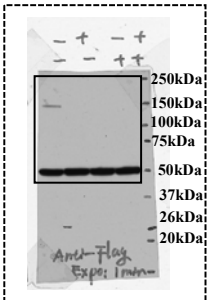

Figure 1c

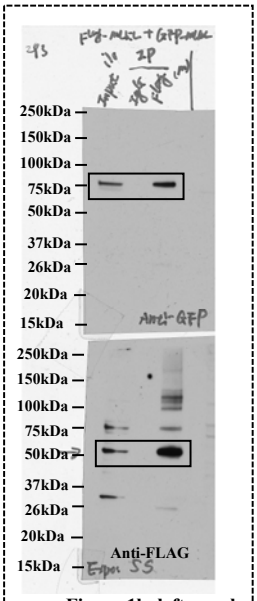

Figure 1b, left panel

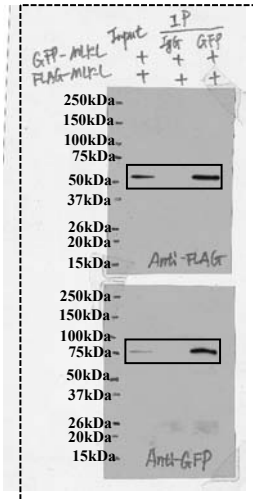

Figure 1b, right panel

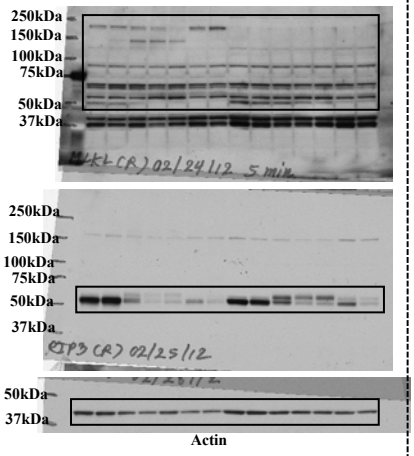

Figure 1d

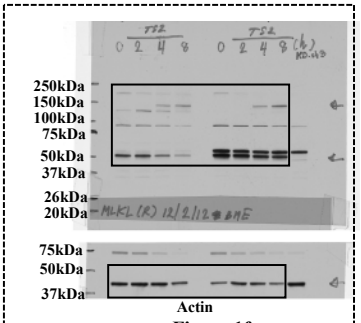

Figure 1f

Supplementary Figure 8 Original scans of western blots. Black boxes indicate cropped region.

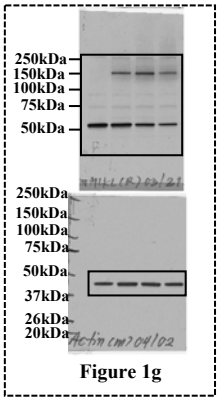

Figure 1g

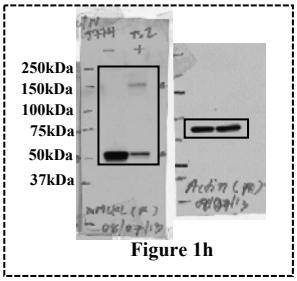

Figure 1h

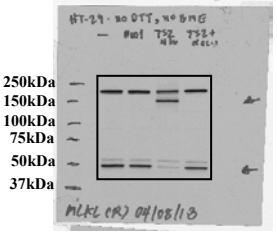

Figure 2a, left panel

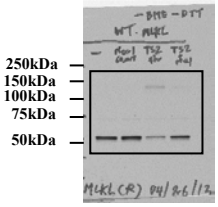

Figure 2a, right panel

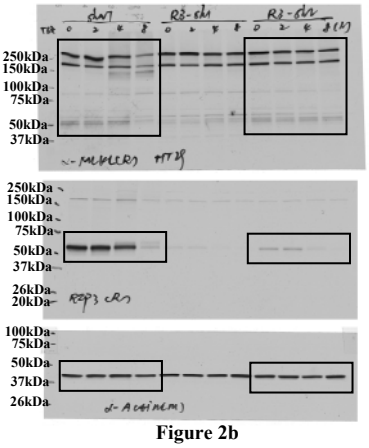

Figure 2b

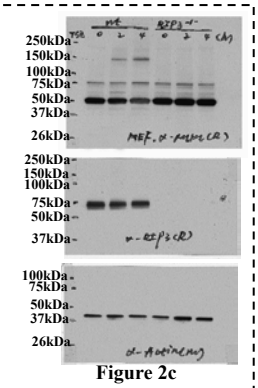

Figure 2c

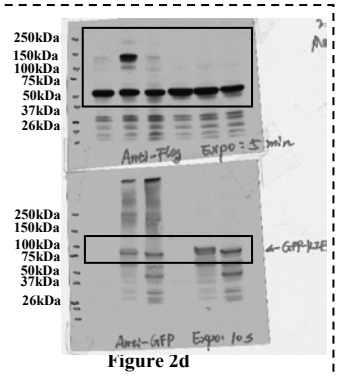

Figure 2d

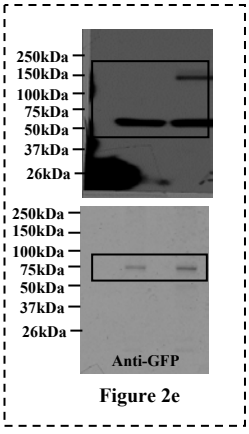

Figure 2e

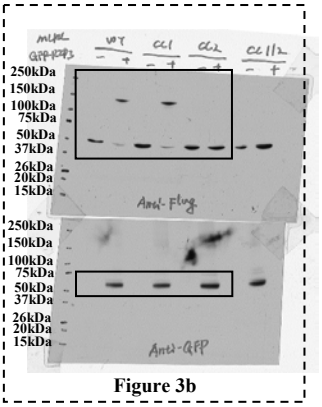

Figure 3b

Supplementary Figure 8 continued

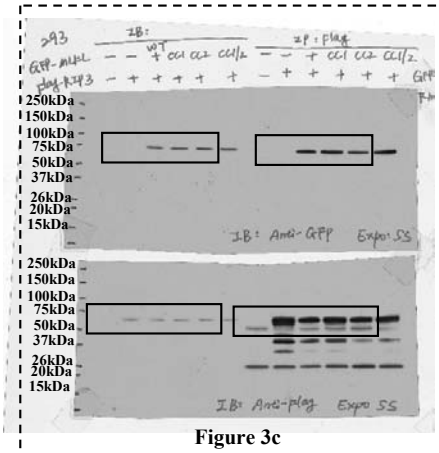

Figure 3c

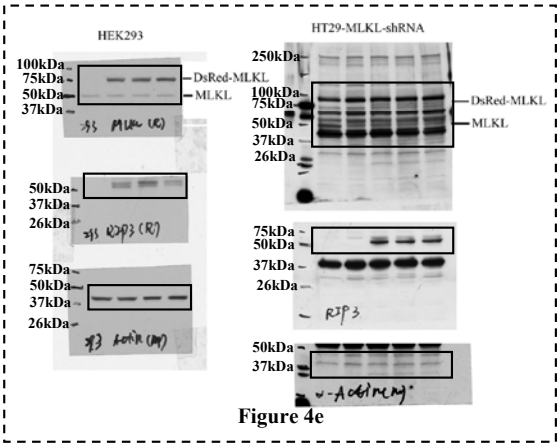

Figure 4e

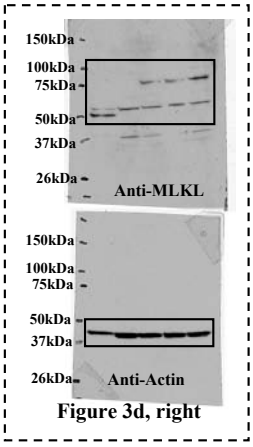

Figure 3d, right

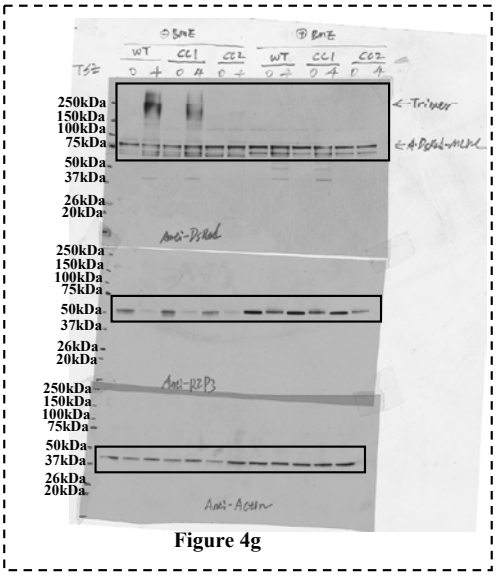

Figure 4g

Supplementary Figure 8 continued

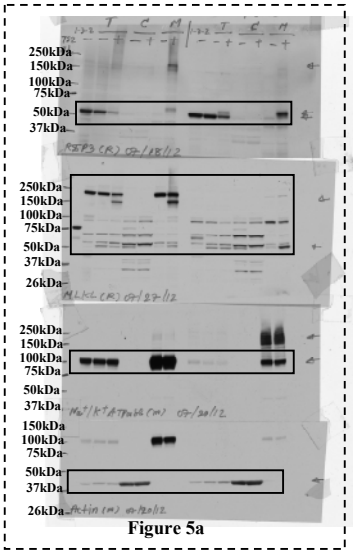

Figure 5a

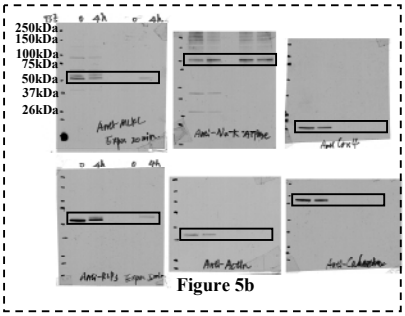

Figure 5b

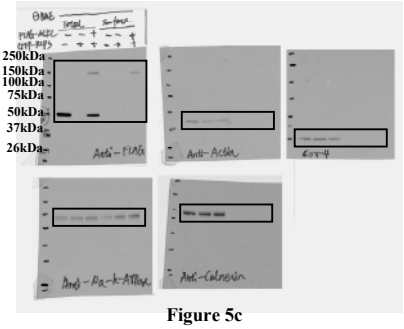

Figure 5c

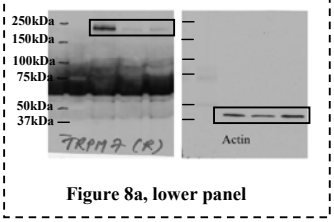

Figure 8a, lower panel

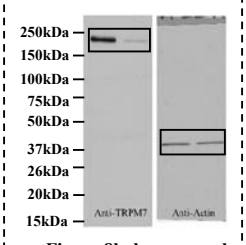

Figure 8b, lower panel

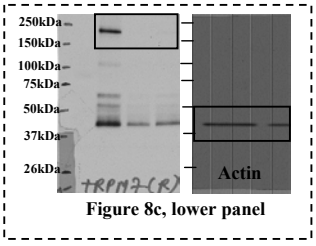

Figure 8c, lower panel

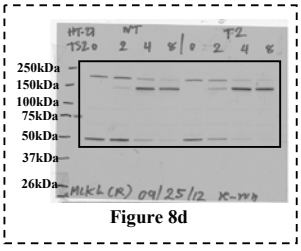

Figure 8d

Supplementary Figure 8 continued

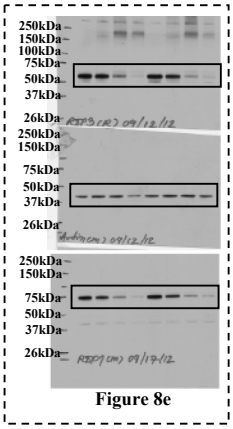

Figure 8e

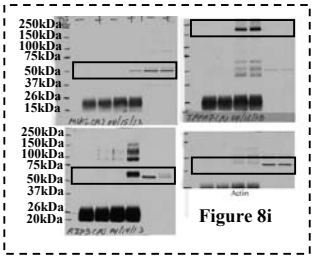

Figure 8i

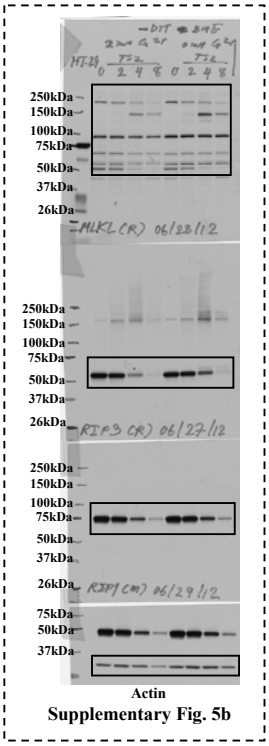

Supplementary Fig. 5b

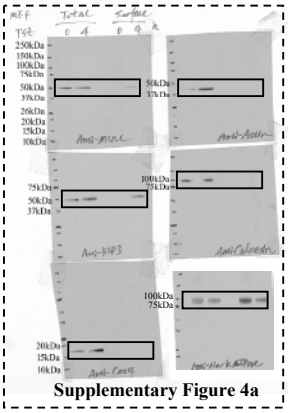

Supplementary Figure 4a

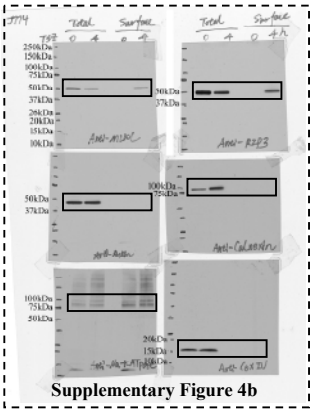

Supplementary Figure 4b

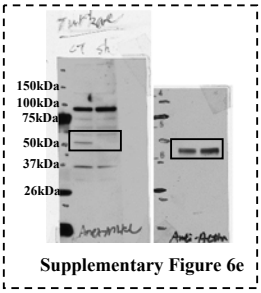

Supplementary Figure 6e

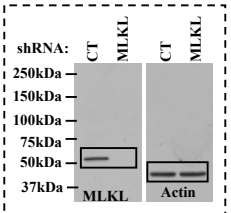

Supplementary Figure 6f

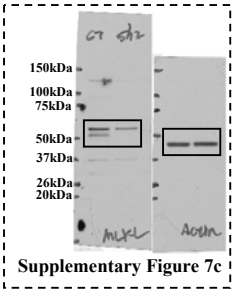

Supplementary Figure 7c

Supplementary Figure 8 continued

Supplementary Table 1 Statistics source data.

Supplementary video 1 Representative time-lapse GCaMP3 fluorescence imaging of control-shRNA HT29 cells treated with TSZ for 8 hours. Left, GFP channel; Middle, differential interference contrast channel (DIC); Right, Merged two channels.

Supplementary video 2 Representative time-lapse GCaMP3 fluorescence imaging of TRPM7-sh#1RNA HT29 cells treated with TSZ for 8 hours. Left, GFP channel; Middle, differential interference contrast channel (DIC); Right, Merged two channels.

Supplementary video 3 Representative time-lapse GCaMP3 fluorescence imaging of control-shRNA HT29 cells cultured in calcium free DMEM and treated with TSZ for 8 hours. Left, GFP channel; Middle, differential interference contrast channel (DIC); Right, Merged two channels.